Serotonin engages an anxiety and fear-promoting circuit in the extended amygdala

Catherine A. Marcinkiewcz[1*], Christopher M. Mazzone[1,2*], Giuseppe D'Agostino[3]. Lindsay R. Halladay[4], J. Andrew Hardaway[1], Jeffrey F. DiBerto[1], Montserrat Navarro[5], Nathan Burnham[5], Claudia Cristiano[3], Cayce E. Dorrier[1], Gregory J. Tipton[1], Charu Ramakrishnan[6], Tamas Kozicz[7,8], Karl Deisseroth[6], Todd E. Thiele[1,5], Zoe A. McElligott[1,9], Andrew Holmes[4], Lora K. Heisler[3] and Thomas L. Kash[1,2,5,10]

[1]Bowles Center for Alcohol Studies, University of North Carolina at Chapel Hill, Chapel Hill, NC 27599, USA

[2]Curriculum in Neurobiology, School of Medicine, University of North Carolina at Chapel Hill School of Medicine, Chapel Hill, NC 27599, USA.

[3]Rowett Institute of Nutrition and Health, University of Aberdeen, Aberdeen AB25 2ZD, UK

[4]National Institute on Alcohol Abuse and Alcoholism, National Institutes of Health, Rockville, MD 20852-9411, USA

[5]Department of Psychology & Neuroscience, College of Arts and Sciences, University of North Carolina at Chapel Hill, Chapel Hill, NC 27599, USA

[6]Department of Bioengineering, Stanford University, Stanford CA 94305, USA

[7]Hayward Genetics Center, Tulane University, New Orleans, LA 70112, USA

[8]Department of Anatomy, Radboud University Nijmegen Medical Center, 6500HB Nijmegen, The Netherlands

[9]Department of Psychiatry, School of Medicine, University of North Carolina at Chapel Hill, Chapel Hill, NC 27599, USA

[10]Department of Pharmacology, School of Medicine, University of North Carolina at Chapel Hill, Chapel Hill, NC 27599, USA

[*]These authors contributed equally to this work

Running Title: 5-HT^{DRN} → CRF^{BNST} elicits fear and anxiety

33

34 **Please address all correspondence to:**

35 Thomas L. Kash
36 Bowles Center for Alcohol Studies
37 University of North Carolina at Chapel Hill
38 CB# 7178 Thurston Bowles Building
39 Chapel Hill, NC 27599-7178
40 Email: tkash@email.unc.edu
41

42 **Keywords:** Serotonin, BNST, anxiety, fear, 5-HT_{2C} receptor, CRF, VTA

43 **Summary paragraph:**

44 Serotonin (5-hydroxytryptamine; 5-HT) is a neurotransmitter that has an essential role in the
45 regulation of emotion. The precise circuits through which aversive states are orchestrated by 5-
46 HT, however, have not yet been defined. Here we show that 5-HT from the dorsal raphe nucleus
47 (5-HT^{DRN}) enhances fear and anxiety and activates a subpopulation of corticotropin-releasing
48 factor (CRF) neurons in the bed nucleus of the stria terminalis (CRF^{BNST}). Specifically, 5-HT^{DRN}
49 projections to the BNST, via actions at 5-HT_{2C} receptors (5-HT_{2C}Rs), engage a CRF^{BNST}
50 inhibitory microcircuit that silences anxiolytic BNST outputs to the ventral tegmental area
51 (VTA) and lateral hypothalamus (LH). Further, we demonstrate that this CRF^{BNST} inhibitory
52 circuit underlies aversive behavior following acute exposure to selective serotonin reuptake
53 inhibitors (SSRIs). This early aversive effect is mediated via the corticotrophin releasing factor
54 type 1 receptor (CRF_1R) given that CRF_1R antagonism is sufficient to prevent acute SSRI-
55 induced enhancements in aversive learning. These results reveal an essential 5-HT^{DRN}
56 $\rightarrow CRF^{BNST}$ circuit governing fear and anxiety and provide a potential mechanistic explanation
57 for the clinical observation of early adverse events to SSRI treatment in some patients with
58 anxiety disorders[1,2].

59 In view of multiple converging lines of evidence pinpointing 5-HT as a critical
60 neuromodulator of pathological fear learning[3,4], we first interrogated the endogenous recruitment
61 of the 5-HT$^{DRN \rightarrow BNST}$ circuit by an aversive footshock stimulus. Using fluorogold to retrogradely
62 label BNST-projecting 5-HT neurons in the DRN, we found that c-fos, an immediate early gene
63 indicative of *in vivo* neuronal activation, was significantly elevated in 5-HT$^{DRN \rightarrow BNST}$ neurons
64 after footshock (Figure 1a-f). Using *in vivo* electrophysiology, we then probed the neuronal
65 dynamics of the BNST during fear conditioning and recall and found evidence for engagement
66 during both conditioning and recall (Extended Data Figure 1).

67 To decipher the role of this 5-HT$^{DRN \rightarrow BNST}$ circuit in aversive behavior,
68 Channelrhodopsin2 (ChR2)-eYFP was selectively expressed in 5-HT^{DRN} neurons through the
69 delivery of a Cre-inducible viral vector in mice expressing Cre recombinase under the control of
70 a serotonin transporter promoter (*Sert^{Cre}*) for both *in vivo* and *ex vivo* analysis. We observed
71 eYFP+ (5-HT) cell bodies in the DRN and eYFP+ fibers in both the dorsal and ventral aspects of
72 the BNST (*Sert^{Cre}*::ChR2$^{DRN \rightarrow BNST}$), confirming a direct projection of 5-HT neurons originating
73 in the DRN to the BNST (Figure 1g-h)[5]. Optical stimulation of these fibers in BNST slices
74 evoked 5-HT release, as measured by fast-scan cyclic voltammetry (FSCV) (Figure 1i-j).
75 Furthermore, bath application of the SSRI fluoxetine reliably decreased the rate of 5-HT
76 reuptake, confirming that photostimulation of SERT+ terminals in the BNST originating from
77 the DRN induces 5-HT release (Figure 1k-l).

78 We next examined whether this 5-HT$^{DRN \rightarrow BNST}$ circuit is functionally relevant for fear and
79 anxiety-like behavior. To investigate this, *Sert^{Cre}*::ChR2$^{DRN \rightarrow BNST}$ mice were implanted with
80 bilateral optical fibers and photostimulated in the BNST (473 nm, 20 Hz) using a standard tone-
81 shock fear conditioning paradigm. Optogenetic stimulation of this pathway was paired with a

82 tone that co-terminated with a scrambled footshock. Cued fear was assessed 24 hours after, and
83 contextual fear 48 hours after, the initial fear acquisition session (Figure 1m-n). While no
84 changes were observed during fear acquisition, both cued and contextual fear recall were
85 significantly heightened in photostimulated $Sert^{Cre}$::$ChR2^{DRN \rightarrow BNST}$ mice (Figure 1o-q). We next
86 assessed anxiety-like behavior using well-characterized assays, the elevated plus maze (EPM)
87 and novelty-suppressed feeding (NSF) tests. Upon stimulation with light, $Sert^{Cre}$::$ChR2^{DRN \rightarrow BNST}$
88 mice exhibited enhanced anxiety-like behavior in both the EPM and NSF (Figure 1r-s and
89 Extended Data Figure 2a-b). Importantly, photostimulation did not induce hypolocomotion in the
90 EPM or open field tests nor did it alter home-cage feeding, thus confirming that hypophagia in
91 the NSF assay was due to anxiety and not a reduction in appetitive drive (Extended Data Figure
92 2c-e). One potential explanation of these results is that terminal stimulation in the BNST
93 produces antidromic spikes in DRN cell bodies that release 5-HT in other brain regions, which
94 could be also be driving these behaviors. In light of this, we probed the mechanism more deeply
95 using converging approaches.

96 To determine a receptor target through which 5-HT is signaling in the BNST, we then
97 examined the impact of optogenetically evoked 5-HT^{DRN} release on postsynaptic neuronal
98 excitability and found a 3.05 ± 0.59 mV depolarization that was blocked by a $5\text{-HT}_{2C}R$
99 antagonist (Figure 1t-u). In contrast to previous reports demonstrating co-release of 5-HT and
100 glutamate from DRN projections to the nucleus accumbens[6], we did not observe any time-locked
101 light-evoked EPSCs in the BNST (data not shown). These results indicate that $5\text{-HT}^{DRN \rightarrow BNST}$
102 projections have a predominantly excitatory effect that is dependent on $5\text{-HT}_{2C}R$ signaling. To
103 examine the role of $5\text{-HT}_{2C}R$ containing neurons in anxiety-like behavior, we next took
104 advantage of a $Htr2c^{Cre}$ mouse line (Extended Data Figure 3a-b)[7]. Using Designer Receptors

105 Exclusively Activated by Designer Drugs (DREADDs)[8], we found that activation of G_q signaling
106 in 5-HT_{2C}R-expressing neurons in the BNST significantly delayed the onset of feeding in the
107 NSF assay without impacting home cage feeding behavior (Extended Data Figure 3c-g), thus
108 phenocopying the effect observed with $5\text{-HT}^{DRN\rightarrow BNST}$ fiber stimulation during NSF. Taken
109 together, these results provide converging evidence that activation of $5\text{-HT}^{DRN\rightarrow BNST}$ inputs
110 elicits anxiety-like behavior via 5-HT_{2C}R signaling.

111 We then considered the neurochemical phenotype of these target $5\text{-HT}^{DRN\rightarrow}5\text{-HT}_{2C}R^{BNST}$
112 neurons and hypothesized that 5-HT via 5-HT_{2C}R modulates the activity of neurons expressing
113 the neuropeptide CRF. This hypothesis was based upon a previous analysis of 5-HT_{2C}R
114 knockout mice, which exhibit an anxiolytic phenotype associated with a reduction of c-fos in
115 CRF^{BNST} neurons[9]. Initially, using CRF reporter mice to *a priori* select CRF neurons for
116 recordings, we found a heterogeneous 5HT-induced response of CRF^{BNST} (Extended Data Figure
117 4a), with only a subset demonstrating a depolarization. Consistent with this, double fluorescence
118 *in situ* hybridization revealed that only a subset of CRF neurons within the dorsal BNST (~70%)
119 and ventral BNST (~43%%) express 5-HT_{2C}Rs (Extended Data Figure 4b-d).

120 While CRF signaling within the BNST is classically associated with anxiety-like
121 behavior[10,11], more recent studies using circuit-based tools have found that optogenetic
122 stimulation of GABAergic projections (which include CRF^{BNST} neurons) to the VTA are
123 anxiolytic[12]. This led us to hypothesize the existence of functionally distinct subsets of CRF^{BNST}
124 neurons that gate different behaviors and are differentially sensitive to 5HT. We used fluorescent
125 retrograde tracer beads to label CRF^{BNST} neurons as VTA-projecting or non-VTA-projecting
126 (Figure 2a) and found that VTA-projecting CRF neurons ($CRF^{BNST\rightarrow VTA}$ neurons) were
127 hyperpolarized by an average of 5.73 ± 1.24 mV and non-VTA-projecting CRF neurons were

128 depolarized by an average of 2.74 ± 0.39 mV during 5-HT bath application. Moreover, the
129 excitatory response to 5-HT in non-VTA-projecting CRF neurons was reversed in the presence
130 of a 5-HT_{2C} receptor antagonist (Figure 2b). Furthermore, all $CRF^{BNST \rightarrow VTA}$ neurons were non-
131 responsive to the 5-HT_2R agonist meta-Chlorophenylpiperazine (mCPP), while all non-VTA
132 projecting CRF neurons were depolarized by mCPP by an average of 3.78 ± 1.17 mV (Extended
133 Data Figure 4e-h). These findings suggest an anatomically distinct response to 5-HT by different
134 subsets of CRF^{BNST} neurons. The subset of CRF^{BNST} neurons expressing $5\text{-HT}_{2C}Rs$ do not
135 project to the VTA and are depolarized by 5-HT, whereas the $CRF^{BNST \rightarrow VTA}$ neurons are
136 hyperpolarized by 5-HT, via actions at another 5-HT receptor.

137 To determine if this 5-HT-dependent mechanism extended to other anxiolytic efferents,
138 we injected retrograde tracer beads into the lateral hypothalamus (LH) of CRF reporter mice and
139 found 5-HT had similar bidirectional effects on non-LH and LH projecting CRF^{BNST} neurons
140 (Extended Data Figure 5a-c). Noting the functional similarities between these two populations,
141 we used retrograde tracing to determine that roughly ~58% of CRF^{BNST} neurons have projections
142 to the LH or VTA (Extended Data Figure 5d-f). Notably, ~20-31% of these CRF^{BNST} output
143 neurons form parallel projections to these structures.

144 In light of recent reports that CRF^{BNST} neurons are exclusively GABAergic[13], we
145 hypothesized that non-VTA-projecting CRF^{BNST} neurons may locally inhibit BNST→VTA
146 neurons to promote fear and anxiety. To test this hypothesis, we injected Crf^{Cre} mice with a Cre-
147 inducible ChR2 into the BNST and retrograde tracer beads into the VTA. We then recorded
148 light-evoked IPSCs from non-ChR2 (ChR2-negative, retrograde tracer-positive) VTA-projecting
149 BNST neurons (Figure 2c). Photostimulation produced action potentials in CRF^{BNST} neurons and
150 light-evoked IPSCs in non-ChR2 VTA-projecting neurons, indicating that CRF^{BNST} neurons form

151 local GABAergic synapses with BNST neurons that project to the VTA. Repeating these same
152 experiments in *Crf*^{CRE}::ChR2^{BNST} mice with retrograde tracer beads in the LH, we found that we
153 could light-evoke GABA currents in LH projecting neurons as well (Extended Data Figure 5g-i).
154 Moreover, we observed that 5-HT increased GABAergic transmission on to BNST→VTA
155 projecting neurons in a tetrodotoxin and 5-HT$_{2C}$R antagonist dependent manner (Figure 2d-f and
156 Extended Data Figure 5j-n). Similar effects of 5-HT on GABAergic transmission were found in
157 BNST→LH projecting neurons (Extended Data Figure 5o-v). Furthermore, slice recordings in a
158 CRF reporter line indicates that 5-HT does not increase GABAergic transmission on to the
159 general population of CRF^{BNST} neurons nor does it directly excite non-CRF VTA projecting
160 neurons (Extended Data Figure 6). The 5-HT$_2$R agonist mCPP also increased GABAergic but
161 not glutamatergic transmission in the BNST (Extended Data Figure 7). Finally, to test if
162 optically evoked 5-HT can inhibit BNST outputs to the VTA, we performed slice recordings in
163 the BNST of *Sert*^{Cre}::ChR2$^{DRN→BNST}$ mice and found that brief photostimulation of 5-HT
164 terminals in the BNST increased sIPSCs on to VTA projecting BNST neurons in a manner
165 similar to bath applied 5-HT (Extended Data Figure 8a-c). Together, these experiments indicate
166 that CRF^{BNST} neurons inhibit at least two major BNST outputs to the VTA and LH that are
167 reported to be anxiolytic [12,14], providing mechanistic insight into the aversive actions of 5-HT
168 signaling in the BNST.

169 We next took advantage of an intersectional strategy for direct visualization of these non
170 projecting, putatively local CRF^{BNST} neurons[15]. By coupling retrograde Cre-dependence flpases
171 (HSV-LSL1-mCherry-IRES-flpo) in the VTA and LH with INTRSECT(Cre$_{on}$/flp$_{off}$)-Chr2-eYFP
172 in the BNST of *Crf*^{cre} mice (*Crf*^{Cre}::Intrsect-ChR2^{BNST} mice), we were able to genetically isolate
173 non-VTA/LH projecting CRF neurons in the BNST. We also infused Cre-dependent HSV-

174 mCherry vector in a subset of *Crf*^{Cre}::Intrsect-ChR2^{BNST} mice as a control. In HSV-flp infused
175 *Crf*^{Cre}::Intrsect-ChR2^{BNST} mice, we observed a significant reduction in YFP+ cells in the ventral
176 BNST (Extended Data Figure 8d-f), indicating that a large proportion of VTA and LH-projecting
177 CRF^{BNST} neurons are located in the ventral BNST. We also found that 5-HT robustly depolarized
178 these *Crf*^{Cre}::Intrsect-ChR2^{BNST} neurons compared to CRF neurons at large (Figure 2g-i).
179 Furthermore, we observed light evoked IPSCs in the BNST of *Crf*^{Cre}::Intrsect-ChR2^{BNST} mice,
180 confirming local GABA release from these neurons (Extended Data Figure 8g). These results
181 support the existence of a separate population of local CRF^{BNST} neurons that is excited by 5-HT
182 and increases local GABAergic transmission in the BNST, distinct from a population of
183 CRF^{BNST} neurons that project to and release GABA in the VTA or the LH (Extended Data Figure
184 8h-j).

185 To probe the translational relevance of these BNST microcircuits, we adopted a
186 pharmacological approach using SSRIs. SSRIs represent one of the most widely used classes of
187 drugs for psychiatric disorders. One limitation of SSRIs is that acute administration can lead to
188 negative behavioral states[1,2], a finding that is recapitulated in rodent models[3,16–20]. Importantly,
189 the BNST has been demonstrated to be an anatomical site of action for some of the aversive
190 actions of SSRIs in rodents[4]. This provided the opportunity to test our model that 5-HT in the
191 BNST drives aversive behavior through inhibition of BNST outputs to the VTA. We observed
192 that an acute systemic injection of the SSRI fluoxetine increased GABAergic transmission on to
193 VTA projecting neurons in the BNST (Figure 3a-d). We then interrogated the role of CRF^{BNST}
194 neurons in acute fluoxetine-enhanced anxiety using *Crf*^{CRE} mice transduced in the BNST with the
195 Cre-inducible Gi-coupled DREADD. We found that acute fluoxetine potentiated anxiety-like

196 behavior, and this effect was blocked by chemogenetic inhibition of CRF^{BNST} neurons (Figure
197 3e-h).

198 To evaluate directly whether endogenous 5-HT acts on CRF^{BNST} neurons to enhance cued
199 fear memory, we used the same chemogenetic approach to silence CRF^{BNST} neurons during
200 fluoxetine treatment and subsequent fear conditioning (Figure 3i). Chemogenetic inhibition of
201 CRF^{BNST} neurons also significantly attenuated fluoxetine-induced enhancement of cued fear
202 recall, providing proof of concept that augmentation of 5-HT via acute SSRI treatment recruits
203 CRF^{BNST} neurons to enhance fear-related behavior (Figure 3j-k). Next, using connectivity based
204 chemogenetic approaches; we tested whether inhibition of BNST outputs to the VTA and LH is a
205 critical component of 5-HT→BNST-induced aversive states. We observed that activation of G_q
206 signaling in VTA- and LH-projecting BNST neurons, targeted by HSV-Cre-eYFP infused in the
207 VTA and LH and Cre-dependent Gq-coupled DREADD infused in the BNST
208 (HSV^{Cre}::$hM3Dq^{BNST}$), significantly attenuated fluoxetine enhancement of cued fear recall
209 (Figure 3l-o). Together, these data provide compelling evidence that acute fluoxetine engenders
210 aversive behavior by recruiting CRF neurons in the BNST that in turn inhibit putative
211 GABAergic (anxiolytic and stress buffering) outputs from the BNST to the VTA and LH.
212 Pharmacological interventions that target this circuit may improve adverse symptoms during the
213 initial weeks of SSRI treatment. Based on the critical role for CRF^{BNST} neurons in fluoxetine
214 induced aversive behavior, we examined the impact of a systemic CRF_1R antagonist on SSRI
215 enhancement of cued fear recall. Notably, blocking the CRF system reduced this aversive state
216 and abolished the increase in sIPSCs in LH-projecting neurons in the BNST during bath
217 application of 5-HT (Extended Data Figure 9). This provides translational evidence that CRF_1R
218 antagonists given in concert with SSRIs could be a promising treatment for anxiety disorders.

219 Taken together, these data reveal a discrete 5-HT responsive circuit in the BNST that
220 underlies pathological anxiety and fear associated with a hyperserotonergic state (Extended Data
221 Figure 10). SSRIs are currently a first-line treatment for anxiety and panic disorders but can
222 acutely exacerbate symptoms, resulting in poor therapeutic compliance. Our results strongly
223 implicate 5-HT engagement of a local BNST inhibitory microcircuit in acute SSRI induced
224 aversive behaviors in rodents, and could potentially be involved in the early adverse events seen
225 in clinical populations, emphasizing the need to identify compounds that selectively target both
226 genetically-defined and pathway-specific cell populations.
227
228

229 **REFERENCES**

230 1. Gorman, J. *et al*. An open trial of fluoxetine in the treatment of panic attacks. *J. Clin.*
231 *Psychopharmacol.* **7,** 329–332 (1987).

232 2. Westenberg, H. G. M. & den Boer, J. Serotonin-influencing drugs in the treatment of
233 panic disorder. *Psychopathology* **22,** 68–77 (1989).

234 3. Burghardt, N. S., Bush, D. E. a, McEwen, B. S. & LeDoux, J. E. Acute selective serotonin
235 reuptake inhibitors increase conditioned fear expression: blockade with a 5-HT(2C)
236 receptor antagonist. *Biol. Psychiatry* **62,** 1111–8 (2007).

237 4. Ravinder, S., Burghardt, N. S., Brodsky, R., Bauer, E. P. & Chattarji, S. A role for the
238 extended amygdala in the fear-enhancing effects of acute selective serotonin reuptake
239 inhibitor treatment. *Transl. Psychiatry* **3,** e209 (2013).

240 5. Phelix, C., Liposits, Z. & Paull, W. Serotonin-CRF interaction in the bed nucleus of the
241 stria terminalis: a light microscopic double-label immunocytochemical analysis. *Brain*
242 *Res. Bull.* **28,** 943–948 (1992).

243 6. Liu, Z. *et al*. Dorsal raphe neurons signal reward through 5-HT and glutamate. *Neuron* **81,**
244 1360–74 (2014).

245 7. Burke, L. K. *et al*. Sex difference in physical activity, energy expenditure and obesity
246 driven by a subpopulation of hypothalamic POMC neurons. *Mol. Metab.* **5,** 245–52
247 (2016).

248 8. Armbruster, B. N., Li, X., Pausch, M. H., Herlitze, S. & Roth, B. L. Evolving the lock to
249 fit the key to create a family of G protein-coupled receptors potently activated by an inert
250 ligand. *Proc. Natl. Acad. Sci. U. S. A.* **104,** 5163–8 (2007).

251 9. Heisler, L. K., Zhou, L., Bajwa, P., Hsu, J. & Tecott, L. H. Serotonin 5-HT(2C) receptors
252 regulate anxiety-like behavior. *Genes. Brain. Behav.* **6,** 491–6 (2007).

253 10. Olive, M. F., Koenig, H. N., Nannini, M. a. & Hodge, C. W. Elevated extracellular CRF
254 levels in the bed nucleus of the stria terminalis during ethanol withdrawal and reduction
255 by subsequent ethanol intake. *Pharmacol. Biochem. Behav.* **72,** 213–220 (2002).

256 11. Huang, M. M. *et al*. Corticotropin-releasing factor (CRF) sensitization of ethanol
257 withdrawal-induced anxiety-like behavior is brain site specific and mediated by CRF-1
258 receptors: relation to stress-induced sensitization. *J. Pharmacol. Exp. Ther.* **332,** 298–307
259 (2010).

260 12. Jennings, J. H. *et al*. Distinct extended amygdala circuits for divergent motivational states.
261 *Nature* **496,** 224–8 (2013).

262 13. Dabrowska, J. *et al*. Neuroanatomical evidence for reciprocal regulation of the
263 corticotrophin-releasing factor and oxytocin systems in the hypothalamus and the bed
264 nucleus of the stria terminalis of the rat: Implications for balancing stress and affect.
265 *Psychoneuroendocrinology* **36,** 1312–26 (2011).

266 14. Kim, S.-Y. *et al*. Diverging neural pathways assemble a behavioural state from separable
267 features in anxiety. *Nature* **496,** 219–23 (2013).

268 15. Fenno, L. E. *et al*. Targeting cells with single vectors using multiple-feature Boolean
269 logic. *Nat*. *Methods* **11,** 763–72 (2014).

270 16. Dekeyne, a, Denorme, B., Monneyron, S. & Millan, M. . Citalopram reduces social
271 interaction in rats by activation of serotonin (5-HT)2C receptors. *Neuropharmacology* **39,**
272 1114–1117 (2000).

273 17. Belzung, C., Le Guisquet, a. M., Barreau, S. & Calatayud, F. An investigation of the
274 mechanisms responsible for acute fluoxetine-induced anxiogenic-like effects in mice.
275 *Behav*. *Pharmacol*. **12,** 151–162 (2001).

276 18. Javelot, H. *et al*. Efficacy of chronic antidepressant treatments in a new model of extreme
277 anxiety in rats. *Depress*. *Res*. *Treat*. **2011,** 531435 (2011).

278 19. Liu, J. *et al*. Acute administration of leptin produces anxiolytic-like effects: A comparison
279 with fluoxetine. *Psychopharmacology (Berl)*. **207,** 535–545 (2010).

280 20. Mombereau, C., Gur, T. L., Onksen, J. & Blendy, J. a. Differential effects of acute and
281 repeated citalopram in mouse models of anxiety and depression. *Int J*
282 *Neuropsychopharmacol* **13,** 321–34 (2010).

283

284

285

286

287

288 **ACKNOWLEDGEMENTS**

289 We acknowledge Bryan Roth for providing DREADD viral constructs and *Sert*^{cre} mice, and
290 Bradford Lowell for providing *Crf*^{cre} mice. We also thank Alberto Lopez, Dan Perron, and
291 Alexis Kendra for technical as sistance with stereotaxic surgeries on mice ,Bram Geenen for
292 technical assistance with immunohistochemistry and Elyse Dankoski for technical assistance
293 with the FSCV. This work was supported by NIH grants AA019454, AA011605 (T.L.K.),
294 the Wellcome Trust (098012) and the Biotechnology and Biological Sciences Research Countil
295 grant (BB/K001418/1) (L.K.H.) and by NIH grant K01AA023555 and the Alcohol Beverage
296 Medical Research Fund (Z.A.M.). C.A.M. was supported by a postdoctoral NIAAA F32
297 fellowship (AA021319-02). C.M.M is supported by a predoctoral NIAAA F31 fellowship
298 (F31AA023440).

299 **AUTHOR CONTRIBUTIONS**

300 C.A.M., C.M.M., G.D., Z.A.M., L.K.H. and T.L.K. designed the experiments. A.H. and J.F.D
301 performed triple label fos/tph/flg staining and image analysis. L.R.H. performed electrode
302 placement surgeries and *in vivo* recordings during fear acquisition and recall. C.A.M. performed
303 stereotaxic surgeries for evoked 5-HT electrophysiology and optogenetic behavior experiments.
304 Z.A.M performed slice FSCV experiments and C.A.M performed evoked 5-HT
305 electrophysiology experiments. C.A.M performed stereotaxic surgeries, behavior and data
306 analysis for $5\text{-HT}^{DRN \rightarrow BNST}$ optogenetic experiments. C.A.M. performed all slice
307 electrophysiology experiments and C.M.M and C.A.M. performed stereotaxic surgeries for these
308 experiments (retrograde tracers, ChR2 infusions, and hM3D and hM4D infusions etc.) C.M.M,
309 performed stereotaxic surgeries for chemogenetic manipulations in CRF^{BNST} neurons that were
310 used in fluoxetine fear conditioning experiments and C.A.M. performed behavior and data

311 analysis. N.M. and J.F.D performed surgeries for chemogenetic manipulations in CRF^{BNST}
312 neurons that were used in fluoxetine anxiety (EZM) assays and N.B. and C.A.M. performed
313 behavior and data analysis. C.M.M. and J.F.D. performed stereotaxic surgeries for
314 HSV^{Cre}::hM3D^{BNST} behavioral manipulations and C.A.M. performed behavior and data analysis.
315 C.M.M. also performed imaging and analysis for optogenetic experiments, chemogenetic, and
316 Intrsect experiments. C.R. and K.D. designed Intrsect viral contructs. G.D. performed surgeries,
317 behavior and data analysis for *htr2c*^{Cre}::hM3D^{BNST} experiments. C.A.M., C.M.M. and T.L.K
318 wrote the manuscript with input from Z.A.M, L.H., J.F.D, J.A.H., G.D., T.T., A.H., L.K.H., T.K.
319

320 **AUTHOR INFORMATION**

321 The authors declare no financial conflict of interest. Correspondence and requests for materials
322 should be addressed to T.L.K. (thomas_kash@med.unc.edu).
323

324 **FIGURE LEGENDS**

325 **Figure 1: Optogenetic identification of a 5-HT$^{DRN→BNST}$ projection that elicits anxiety and**
326 **fear-related behavior**. (a) Experimental timeline for c-fos labeling of 5-HT$^{DRN→BNST}$ neurons
327 following an aversive footshock stimulus. (b) Representative images of fluorogold (blue),
328 tryptophan hydroxylase (violet), and c-fos (green) staining in the DRN for 13 mice. Scale bars:
329 100 µm. (c-f) Histograms depicting the number of double and triple labeled neurons in the DRN
330 of naïve and shocked mice. (c) There were no significant differences in the number of BNST
331 projecting 5-HT^{DRN} neurons between groups. (d-f) Footshock lead to significant elevations in the
332 number of c-fos+ (“activated”) 5-HT neurons (t_{11}=2.975, p<0.05, Student’s unpaired two-tailed
333 t-test, n=7 naïve and n=6 shock mice), c-fos+, fluorogold labeled neurons (t_{11}=2.836, p<0.05,

334 Student's unpaired two-tailed t-test, n=7 naïve and n=6 shock mice), and triple labeled neurons
335 (t_{11}=2.374, $p<0.05$, Student's unpaired two-tailed t-test, n=7 naïve and n=6 shock mice). (g)
336 Experimental configuration for light-evoked FSCV experiments in $Sert^{Cre}$::$ChR2^{DRN \rightarrow BNST}$ mice
337 (h) Coronal images showing ChR2-YFP expression in soma of the DRN and axons of the BNST.
338 Scale bars: 500 µm. (i) Representative color plot of 5-HT release to optical stimulation (blue bar,
339 20 Hz 20 pulses) for 3 mice (j) Representative cyclic voltammogram at peak 5-HT (blue dashed
340 line panel E) for 3 mice. (k) Representative Current vs. Time trace at baseline (black) and
341 following 10 µM fluoxetine (red) for 3 mice. (l) Clearance half-life of 5-HT at baseline (white
342 bar) and following 10 µM fluoxetine (red bar). (t_2=8.43, $p<0.05$, Student's paired two-tailed t-
343 test, n = 3 slices from 3 mice) (m) $Sert^{Cre}$ mice were transduced in the DRN and implanted with
344 bilateral optical fibers in the BNST. (n) Schematic of fear conditioning procedures in
345 $Sert^{Cre}$::$ChR2^{DRN \rightarrow BNST}$ mice. (o-q) Photostimulation during fear acquisition had no effect on
346 freezing behavior during fear learning but increased freezing during cued (t_{17}=2.436, $p<0.05$,
347 Student's unpaired two-tailed t-test, n=10 control, n=9 ChR2) and contextual fear recall
348 (t_{17}=2.271, $p<0.05$, Student's unpaired two-tailed t-test, n=10 control, n=9 ChR2). (r) Light
349 delivery to the BNST reduced open arm time in the EPM (t_{15}=2.79, $p<0.05$, Student's unpaired
350 two-tailed t-test, n=8 control, n=9 ChR2) and (s) increased latency to feed in the NSF (t_{17}=2.19,
351 $p<0.05$, Student's unpaired two-tailed t-test, n=9 control, n=10 ChR2). (t) Action potentials
352 generated by photostimulation in the DRN (5 Hz (top), 10 Hz (middle), 20 Hz (bottom), 473
353 nm). (u) Depolarization in cells (t_8=5.20, $p<0.01$, One-sample t-test, n=9 cells from 4 mice) after
354 photostimulation in the BNST (5 Hz, 10 s, 473 nm) and blockade of this response by 5 µM RS
355 102221 (t_4=2.5, $p>0.05$, One-sample t-test, n=5 cells from 2 mice). Data are mean ± s.e.m.
356 *P<0.05; **P<0.01; ***P<0.001.

357

358 **Figure 2: Serotonin activates a local population of CRF^{BNST} neurons that inhibits outputs to**
359 **the midbrain.** (a) Recording scheme for CRF reporter mice injected with retrograde tracer
360 beads in the VTA. (b) 5-HT depolarizes local CRF neurons (t_5=7.06 , p<0.001, One-sample t-
361 test, n=6 cells from 4 mice) in the BNST while hyperpolarizing $CRF^{BNST \rightarrow VTA}$ neurons (t_6=4.64,
362 p<0.01, One-sample t-test, n=7 cells from 6 mice). Non VTA projecting CRF neurons are
363 hyperpolarized by 5-HT in the presence of the 5-HT_{2C}R antagonist RS102221 (t_4=4.74, p<0.01,
364 One-sample t-test, n=5 cells from 3 mice) ($c_{i\text{-}ii}$) Schematic depicting infusions and recording
365 configuration for *Crf*^{Cre}::ChR2^{BNST} mice injected with retrograde tracer beads in the VTA. (c_{iii})
366 Representative trace of light-evoked IPSC in beaded (i.e. VTA projecting), non-ChR2 expressing
367 neurons in the BNST of *Crf*^{Cre}::ChR2 mice with retrograde tracer beads in the VTA (n=8 cells
368 from 3 mice) and blockade of this response by GABAzine ($F_{11,33}$=53.16, p<0.001, Repeated
369 Measures One-way ANOVA, n=4 cells from 3 mice). (d) Recording scheme for C57BL/6 mice
370 with retrograde tracer beads in the VTA or LH (e) Representative traces of sIPSCs in BNST
371 neurons that project to the VTA before and after 5-HT application for 5 cells from 4 mice (f) Bar
372 graphs showing magnitude of 5-HT effect on average sIPSC frequency in BNST neurons that
373 project to the VTA (t_4=3.257, p<0.05, One-sample t-test, n=5 cells from 4 mice) and in BNST
374 neurons that project to the LH (t_5=3.027, p<0.05, One-sample t-test, n=6 cells from 3 mice) and
375 blockade of these responses by TTX and RS 102221. Effects on amplitude were non-significant.
376 (g) Experimental scheme for experiments with *Crf*^{Cre}::Intrsect-ChR2^{BNST}mice. (h-i,) 5-HT
377 significantly depolarizes non-projecting CRF ("Intrsect") neurons in the BNST (t_6=2.501, p <
378 0.05, One-sample t-test, n=7 cells from 5 mice) and produces a significant change in membrane
379 potential in CRF Intrsect neurons compared to all CRF neurons (t_{26}=2.08, p<0.05, Student's

380 unpaired two-tailed t-test, n=21 cells from 14 mice for experiments in all CRF neurons and n=7
381 cells from 5 mice for *Crf*^{Cre}::Intrsect-ChR2^{BNST} experiments). Data are mean ± s.e.m. *P<0.05;
382 **P<0.01; ***P<0.001. # donates P<0.05 for the Student's unpaired two-tailed t-test between all
383 CRF neurons and CRF Intrsect neurons in panel 2h.
384
385 **Figure 3: Acute fluoxetine elicits aversive behavior by engaging inhibitory CRF circuits in**
386 **the BNST.** (a) Schematic of recording for *in vivo* fluoxetine experiments in CRF reporter mice.
387 (b) Representative traces of sIPSCs in VTA projecting neurons in the BNST for 5 experiments in
388 2 saline-treated mice and 7 experiments in 2 fluoxetine-treated mice. (c-d) Bar graphs showing
389 that fluoxetine increases in sIPSC frequency (t_{10}=2.55, p<0.05, Student's unpaired two-tailed t-
390 test, n=5 cells from 2 saline-treated mice, n=7 cells from 2 fluoxetine-treated mice), but not
391 amplitude (t_{10}=0.4752, p>0.05, Student's unpaired two-tailed t-test, n=5 cells from 2 saline mice,
392 n=7 cells from 2 fluoxetine mice) in VTA projecting neurons in the BNST. (e) Experimental
393 configuration for assessment of anxiety in fluoxetine-treated *Crf*^{Cre}::hM4Di^{BNST} mice and a
394 coronal slice of the BNST expressing hM4Di-mCherry. Scale bar: 100 µm. (f) Confirmatory
395 electrophysiology in the BNST showing hyperpolarization of hM4Di-mCherry-expressing cells
396 following bath application of CNO (t_5=4.32, p<0.01, One-sample t-test, n=6 cells from 4 mice)
397 (g-h) Chemogenetic silencing of CRF neurons attenuates fluoxetine-induced anxiety like
398 behavior on the elevated zero maze ($F_{1,30}$=7.086, p<0.05, Two-way ANOVA, n=10
399 fluoxetine/hM4Di and n=8 for all other groups) without any concomitant locomotor effects. (i)
400 Experimental configuration for fear conditioning experiments in *Crf*^{Cre}::hM4Di^{BNST} mice. (j-k)
401 Chemogenetic silencing of CRF^{BNST} neurons had no effect on freezing behavior during fear
402 learning but prevented fluoxetine enhancement of cued fear recall ($F_{1,17}$=8.73, p<0.01, Two-way

403 ANOVA, n=6 mCherry/vehicle and n=5 per group for all other groups). (l) Experimental
404 configuration for assessment of the role of BNST outputs to the VTA and LH in fluoxetine-
405 induced aversive behavior. (m) Confocal image of the BNST from HSV^{Cre}::hM3Dq^{BNST} mice.
406 Scale bars: 500 µm.. (n-o) Chemogenetic activation of BNST neurons that project to the
407 midbrain did not impact fear acquisition but attenuated fluoxetine induced enhancement of cued
408 fear recall ($F_{1,27}$=7.541, p<0.05, Two-way ANOVA, n=7 vehicle/hM3D and n=8 for all other
409 groups). Data are mean ± s.e.m. *P<0.05; **P<0.01; ***P<0.001.

410

411 **METHODS**

412 **Mice:** Mice were used in all experiments. For experiments involving Cre lines, mice were
413 crossed for several generations to C57 mice before using. All wild-type mice were C57BL/6
414 mice obtained from The Jackson Laboratory (Bar Harbor, ME). For all behavior experiments
415 except those involving *Htr2c*^{Cre} mice, male mice ranging in age from 8-16 weeks were used.
416 Female *Htr2c*^{Cre} mice were used in chemogenetic manipulations. Both male and female mice
417 aged 6-20 weeks were used for slice electrophysiology and anatomical tracing experiments. All
418 behavioral studies or tissue collection for *ex vivo* slice electrophysiology were performed during
419 the light cycle.

420 All behavioral experiments in *Htr2c*^{cre} mice were conducted at the University of Aberdeen and in
421 accordance with the United Kingdom Animals (Scientific Procedures) Act of 1986. All *in vivo*
422 electrophysiology experiments were conducted in accordance with all rules and regulations at the
423 National Institute for Alcohol Abuse and Alcoholism at the National Institutes of Health. All
424 other procedures were conducted in accordance with the National Institutes of Health guidelines

425 for animal research and with the approval of the Institutional Animal Care and Use Committee at
426 the University of North Carolina at Chapel Hill.
427 All animals were group housed on a 12 hour light cycle (lights on at 7 a.m.) with *ad libitum*
428 access to rodent chow and water, unless described otherwise. CRF-*ires*-Cre (*Crf*^{cre}) were
429 provided by Dr. Bradford Lowell (Harvard University) and were previously described[21].
430 C57BL/6J mice were obtained from the Jackson Laboratory (Bar Harbor, ME). To visualize
431 CRF-expressing neurons, *Crf*^{Cre} mice were crossed with either an Ai9 or a cre-inducible L10-
432 GFP reporter line (Jackson Laboratory)[22] to produce CRF-Ai9 or CRF-L10GFP progeny,
433 referred to throughout the manuscript as CRF-reporters. *Sert*^{Cre} mice (from GENSAT) were a
434 generous gift from Dr. Bryan Roth. *Htr2c*^{Cre} mice were supplied by Dr. Lora Heisler and are
435 described in detail elsewhere[7].

436 Male mice were used for *in vivo* optogenetic behavioral experiments and for assessing the
437 involvement of BNST CRF neurons on fluoxetine-induced enhancement of fear. Female 5-HT$_{2C}$-
438 Cre mice were used in chemogenetic manipulations. Both male and female mice were used for
439 slice electrophysiology and anatomical tracing experiments. All behavioral studies or tissue
440 collection for *ex vivo* slice electrophysiology were performed during the light cycle.

441 **Viruses and tracers:** All AAV viruses except INTRSECT constructs were produced by the
442 Gene Therapy Center Vector Core at the University of North Carolina at Chapel Hill and had
443 titers of >10^{12} genome copies/mL. For *ex vivo* and *in vivo* optical experiments, mice were
444 injected with rAAV5-ef1α-DIO-hChR2(H134R)-eYFP or rAAV5-ef1α-DIO-eYFP as a control.
445 Red IX retrobeads (Lumafluor) were used to fluorescently label LH - and VTA-projecting BNST
446 neurons during *ex vivo* slice electrophysiology recordings. The retrograde tracer Fluoro-Gold
447 (Fluorochrome) was used for anatomical mapping. Choleratoxin B (CTB) 555 and CTB 657

448 retrograde tracers (Invitrogen; C34776, and C34778, respectively) diluted to 0.5% (w/v) in
449 sterile PBS were used per injection site for anatomical mapping of collateral projections from
450 BNST to LH and VTA. For chemogenetic manipulations, mice were injected with 400 nl of
451 rAAV8-hsyn-DIO-hM3D(Gq)-mCherry, rAAV8-hsyn-DIO-hM4D(Gi)-mCherry, or rAAV8-
452 hsyn-DIO-mCherry bilaterally. HSV-hEF1α-mCherry, HSV-ef1α-LSL1-mCherry-IRES-flpo,
453 and HSV-ef1α-IRES-Cre (supplied by Rachel Neve at the McGovern Institute for Brain
454 Research at MIT) were injected bilaterally into the VTA and LH at a volume of 500500 nL per
455 sitesite. The INTRSECT construct AAVdj-hSyn-Con/Foff-hChR2(H134R)-EYFP was infused at
456 500 nl per side into the BNST. All AAV constructs had viral titers >10^{12} genome particles/ml.

457 **Stereotaxic injections:** All surgeries were conducted using aseptic technique. Adult mice (2-5
458 months) were deeply anesthetized with 5% isoflurane (vol/vol) in oxygen and placed into a
459 stereotactic frame (Kopf Instruments) while on a heated pad. Sedation was maintained at 1.5-
460 2.5% isoflurane during surgery. An incision was made down the midline of the scalp and a
461 craniotomy was performed above the target regions and viruses and fluorescent tracers were
462 microinjected using a Neuros Hamilton syringe at a rate of 100 nl/min. After infusion, the needle
463 was left in place for 10 minutes to allow for diffusion of the virus before the needle was slowly
464 withdrawn. Injection coordinates (in mm, midline, Bregma, dorsal surface): BNST (±1.00, 0.30,
465 -4.35), LH (±0.9 to 1.10, -1.7, -5.00 to -5.2), VTA (-0.3, -2.9, -4.6), DR (0.0, -4.65, -3.2 with a
466 23° angle of approach). When using retrobeads, injection volumes into the LH and VTA were
467 300 nl and 400 nl, respectively. Fluorogold injection volumes were 200 nl per target site. CTB
468 volumes were 200200 nL per target site. An optical fiber was implanted in the BNST (±1.00,
469 0.20, -4.15) at a 10° angle for *in vivo* photostimulation studies. After fiber implantation, dental
470 cement was used to adhere the ferrule to the skull. Following surgery, all mice returned to group

471 housing. Mice were allowed to recover for at least 3 weeks before being used for chemogenetic
472 behavioral studies, or 6 weeks for *in vivo* optogenetic studies.

473 **Drugs:** RS 102221, 5-HT and mCPP were from Tocris (Bristol, UK). For electrophysiology
474 experiments, RS 102221 was made up to 100 mM in DMSO and then diluted to a final
475 concentration of 5 µM in aCSF. 5-HT and mCPP were stocked at 10 and 20 mM, respectively, in
476 ddH_2O and diluted to their final concentations in aCSF. For electrophysiology experiments,
477 clozapine-N-oxide (CNO; from Dr. Bryan Roth) was stocked at 100 mM in DMSO and diluted
478 to 10 µM in aCSF. For behavior experiments, CNO was dissolved in 0.5% DMSO (in 0.9%
479 saline) to a concentration of 0.1 mg/ml or 0.3 mg/ml and injected at 10 ml/kg for a final
480 concentration of 1 or 3 mg/kg, i.p. Fluoxetine (Sigma) was made up in 0.9% NaCl to a
481 concentration of 1 mg/ml and then injected at 10 ml/kg for a final concentration of 10 mg/kg, i.p.

482 ***In vivo* Electrophysiological Procedures**

483 *Surgical Procedures*

484 Mice were anesthetized with 2% Isoflurane (Baxter Healthcare, Deerfield, IL) and implanted
485 with 2x8 electrode (35um tungsten) micro-arrays (Innovative Neurophysiology Inc, Durham,
486 NC) targeted at the BNST (ML: 0.8 mm, AP: ± 0.5 mm , and DV: -4.15 mm relative to Bregma).
487 Following surgery, mice were singly housed and allowed at least one week to recover prior to
488 behavioral testing.

489 *Fear Conditioning*

490 Fear conditioning took place in 27 × 27 × 11cm conditioning chambers (Med Associates,
491 St. Albans, VT), with a metal-rod floor (Context A) and scented with 1% vanilla. Mice received

492 5 parings of a pure tone CS with a .6mA foot shock. 24 h following conditioning, mice
493 underwent a CS recall test (10 presentations of the CS alone, 5 sec ITI), which was conducted in
494 a Plexiglas cylinder (20cm diameter) and scented with 1% acetic acid (Context B). Stimulus
495 presentations for both tests were controlled by MedPC (Med Associates Inc, St. Albans, VT).
496 Cameras were mounted overhead for recording freezing behavior, which was scored
497 automatically using CinePlex Behavioral Research System software (Plexon Inc, Dallas, TX).

498 *Electrophysiological recording and single unit analysis*

499 Electrophysiological recording took place during both fear conditioning and CS recall tests.
500 Individual units were identified and recorded using Omniplex Neural Data Acquisition System
501 (Plexon Inc, Dallas, TX). Neural data was sorted using Offline Sorter (Plexon Inc, Dallas, TX).
502 Waveforms were isolated manually, using principal component analysis. To be included in the
503 analyses, spikes had to exhibit a refractory period of at least 1 ms. Autocorrelograms from
504 simultaneously recorded units were examined to ensure that no cell was counted twice. Single
505 units were analyzed by generating perievent histograms (3 sec bins) of firing rates from 30 sec
506 prior to CS onset until 30 sec after CS offset (NeuroExplorer 5.0, Nex Technologies, Madison,
507 AL). Firing rates were normalized to baseline (30 sec prior to CS onset) using z-score
508 transformation. Analysis included a total of 139 cells over three days of recording. Data reported
509 for raw firing rates include only putative principal neurons (<10Hz).

510 The formula for computing the suppression ratio was (average freezing rate) / (average freezing
511 rate + average movement rate). Each cell was calculated individually. A value of .5 = no change
512 in rate).

513 ***Ex vivo* Slice Electrophysiology:** Brains were sectioned at 0.07 (mm/s) on a Leica 1200S
514 vibratome to obtain 300 µm coronal slices of the BNST, which were incubated in a heated
515 holding chamber containing normal, oxygenated aCSF (in mM:124 NaCl, 4.4 KCl, 2 $CaCl_2$, 1.2
516 $MgSO_4$, 1 NaH_2PO_4, 10.0 glucose, and 26.0 $NaHCO_3$) maintained at 30 ± 1˚C for at least 1 hour
517 before recording. Slices were transferred to a recording chamber (Warner Instruments)
518 submerged in normal, oxygenated aCSF maintained at 28-30˚C at a flow rate of 2 ml/min.
519 Neurons of the BNST were visualized using infrared differential interference contrast (DIC)
520 video-enhanced microscopy (Olympus). Borosilicate electrodes were pulled with a Flaming-
521 Brown micropipette puller (Sutter Instruments) and had a pipette resistance between 3-6 MΩ.
522 Signals were acquired via a Multiclamp 700B amplifier, digitized at 10 kHz and analyzed with
523 Clampfit 10.3 software (Molecular Devices, Sunnyvale, CA, USA).

524 *Light-evoked action potentials*: In $Sert^{Cre}$ or Crf^{Cre} mice, fluorescently labeled neurons
525 expressing ChR2 were visualized and stimulated with a blue (470 nm) LED using a 1 Hz, 2 Hz, 5
526 Hz, 10 Hz, and 20 Hz stimulation protocol with a pulse width of 0.5 ms. Evoked action
527 potentials were recorded in current clamp mode using a potassium gluconate based internal
528 solution (in mM: 135 K+ gluconate, 5 NaCl, 2 $MgCl_2$, 10 HEPES, 0.6 EGTA, 4 Na_2ATP, 0.4
529 Na_2GTP, pH 7.3, 285–290 mOsmol).

530 *Light-evoked synaptic transmission:* In Crf^{Cre} mice with ChR2 in the BNST and retrograde tracer
531 beads in the VTA or LH, we visualized non-ChR2-expressing, beaded neurons using green (532
532 nm) LED. Recordings were conducted in voltage clamp mode using a cesium-methansulfonate
533 (Cs-Meth) based internal solution (in mM: 135 cesium methanesulfonate, 10 KCl, 1 $MgCl_2$, 0.2
534 EGTA, 2 QX-314, 4 MgATP, 0.3 GTP, 20 phosphocreatine, pH 7.3, 285–290 mOsmol) so that
535 we could detect EPSCs (-55 mV) and IPSCs (+10 mV) in the same neuron. After confirming the

536 absence of a light-evoked EPSC signal, we measured light-evoked IPSCs during a single, 5 ms
537 light pulse of 470 nm. In a subset of these experiments, SR95531 (GABAzine, 10 µM) was bath
538 applied for 10 minutes to block IPSCs.

539 *Drug effects in CRF^{BNST} neurons: Crf*-reporter mice were injected with retrograde tracer beads
540 into the VTA (ML -0.5, AP -2.9, DV -4.6). We then recorded from beaded (VTA-projecting) and
541 non-beaded (non-projecting) CRF neurons in the BNST. Acute drug effects were determined in
542 current clamp mode in the presence of TTX using a potassium gluconate-based internal solution.
543 After a 5-minute stable baseline was established, 5HT (10 µM) or mCPP (20 µM) was bath
544 applied for 10 minutes while recording changes in membrane potential. The difference in
545 membrane potential between baseline and drug application at peak effect (delta or Δ MP) was
546 later determined. In a subset of mCPP experiments, slices were incubated with RS 102221 (5
547 µM) for at least 20 minutes before experiments began.

548 *Synaptic transmission:* Spontaneous inhibitory postsynaptic currents (sIPSCs) were assessed in
549 voltage clamp using a potassium-chloride gluconate-based intracellular solution (in mM: 70 KCl,
550 65 K^+-gluconate, 5 NaCl, 10 HEPES, 0.5 EGTA, 4 ATP, 0.4 GTP, pH 7.2, 285–290 mOsmol).
551 IPSCs were pharmacologically isolated by adding kynurenic acid (3 mM) to the aCSF to block
552 AMPA and NMDA receptor-dependent postsynaptic currents. The amplitude and frequency of
553 sIPSCs were determined from 2 minute recording episodes at -70 mV. The baseline was
554 averaged from the 4 minutes preceding the application of 5-HT (10 µM) or mCPP (10 µM) for
555 10 minutes. In a subset of these experiments, RS 102221 (5 µM) was added to the aCSF and
556 slices were incubated in this drug solution for at least 20 minutes before experiments began. For
557 miniature IPSCs (mIPSCs), TTX was included in the aCSF to block network activity.

558 In *Sert*^{Cre}::ChR2^{BNST} mice with retrograde tracer beads in the VTA, sIPSCs were recorded as
559 described above. After achieving a stable baseline, a 10 s, 20 Hz photostimulation was applied.

560 For assessment of spontaneous excitatory postsynaptic currents (sEPSCs), a cesium gluconate-
561 based intracellular solution was used (in mM: 135 Cs^{+}-gluconate, 5 NaCl, 10 HEPES,
562 0.6 EGTA, 4 ATP, 0.4 GTP, pH 7.2, 290–295 mOsmol). $AMPA_R$-mediated EPSCs were
563 pharmacologically isolated by adding 25 μM picrotoxin to the aCSF. sEPSC recordings were
564 acquired in 2 minute recording blocks at -70 mV.

565 **Fast-scan cyclic voltammetry (FSCV):** Electrodes were fabricated as previously described and
566 cut to 50-100 um in length[23]. Animal and slice preparation were as described above for
567 electrophysiology and slices were perfused on the rig in ACSF. Using a custom built potentiostat
568 (University of Washington Seattle), 5-HT recordings were made in the BNST using TarHeel CV
569 written in lab view (National Instruments). Briefly a triangular waveform (-0.1 V to 1.3 V with a
570 10% phase shift at 1000 V/s, vs. Ag/AgCl) was applied to the carbon fiber electrode at a rate of
571 10 Hz. Slices were optically stimulated with 20 5-ms blue (490 nm) light pulses at a rate of 20
572 Hz down the submerged 40x objective. 10 cyclic voltammograms were averaged prior to optical
573 stimulation for background subtraction. Voltammograms were digitally smoothed one time with
574 a fast Fourier transform following data collection and analyzed with HDCV (UNC Chapel Hill).
575 Fluoxetine (10 μM) was bath applied following a stable baseline (20 minutes).

576

577 **Behavioral Assays:**

578 For chemogenetic manipulations, mice were transported to a holding cabinet adjacent to the
579 behavioral testing room to habituate for at least 30 minutes before being pretreated with CNO (3

580 mg/kg, i.p. for *Crf*^{Cre} mice and 1 mg/kg, i.p. for *Htr$_{2C}$*^{Cre} mice). All behavior testing began 45
581 minutes following CNO treatment, with the exception of fear conditioning training, which
582 occurred 30 minutes after a CNO injection. When assessing the effect of fluoxetine on fear
583 conditioning, fluoxetine (10 mg/kg, i.p.), or vehicle, was administered 1 hour before training (30
584 minutes before CNO treatment). For optogenetic manipulations, mice received bilateral
585 stimulation (473 nm, ~10 mW, 5 ms pulses, 20 Hz) when specified. Unless specified, all
586 equipment was cleaned with a damp cloth between mouse trials. All sessions were video
587 recorded and analyzed using EthoVision software (Noldus Information Technologies) except
588 where noted.

589 *Elevated Plus Maze:* Mice were placed in the center of an elevated plus maze and allowed to
590 explore during a 5 minute session. Light levels in the open arms were ~14 lux. During
591 optogenetic manipulations mice received bilateral stimulation during the entire 5 minute session.
592 Mice that left the maze were excluded from analysis (n= 2 control, 1 ChR2 from optogenetic
593 experiments).

594 *Open Field:* Mice were placed into the corner of a white Plexiglas open field arena (25 x 25 x 25
595 cm) and allowed to freely explore for 30 minutes. The center of the open field was defined as the
596 central 25% of the arena. For optogenetic studies the 30 minute session was divided into three
597 10-minute epochs consisting of stimulation off, stimulation on, and stimulation off periods.

598 *Novelty-Induced Suppression of Feeding:* 48 hours prior to testing mice were provided with
599 access to a single piece of Froot Loops cereal (Kellogg's) in their home cage. 24 hours prior to
600 testing, home cage chow was removed and mouse body weights were recorded. Water remained
601 available *ad lib*. Beginning at least one hour before testing mice transferred to new clean cages

602 so they were singly housed for the test session and body weights were recorded. During the test
603 session mice were placed into an arena (25x25x25 cm) that contained a single Froot Loop on top
604 of a piece of circular filter paper. Mice were monitored by a live observer and the latency for the
605 mouse to begin eating the pellet was measured, allowing up to 10 minutes. All mice began eating
606 within this time. Following the initiation of feeding, mice were removed from the arena and
607 placed back into their home cages. Mice were then provided with 10 minutes of access to a pre-
608 weighed amount of Froot Loops™ for a post-test feeding session. After this 10 minute post-test,
609 the remaining Froot Loops were weighed and mice were returned to *ad lib* home cage chow.
610 Mice were returned to group housing at the end of this session. For optogenetic experiments,
611 mice received constant 20 Hz optical stimulation during both the latency to feed assay and the 10
612 minute post-test. During optogenetic experiments, one control mouse did not feed during the 10
613 minute NSF session and was excluded from the results.

614 *Home cage feeding: Sert^{Cre}* mice were food deprived for 24 hours. On the day of the experiment,
615 mice were acclimated to the behavior room for 1 hour. A single preweighed food pellet was
616 placed in the home cage and the mice were allowed to eat for 10 minutes during optogenetic
617 stimulation. At the end of the experimental session, the pellet was removed and weighed and
618 mice were given *ad lib* access to food.

619 Htr_{2C}^{Cre} mice were acclimated in metabolic chambers (TSE Systems, Germany) for 2 days before
620 the start of the recordings. After acclimation, mice were food deprived for 24 hours. Following
621 fasting, mice received an IP injection of CNO 30 minutes before food presented again. Mice
622 were recorded for 12 hours with the following measurements being taken every 30 minutes:
623 water intake, food intake, ambulatory activity (in X and Z axes), and gas exchange (O_2 and CO_2)

624 (using the TSE LabMaster system, Germany). Energy expenditure was calculated according to
625 the manufacturer's guidelines (PhenoMaster Software, TSE Systems).

626 *Fear Conditioning:* We used a three day protocol to assess both cued and contextual fear recall.
627 On the first day, mice were placed into a fear conditioning chamber (Med Associates) that
628 contained a grid floor and was cleaned with a scented paper towel (19.5% EtOH, 79.5% H2O,
629 1% vanilla). After a 3 minute baseline period, mice were exposed to a 30 second tone (3 KHz, 80
630 dB) that co-terminated with a 2 second scrambled foot shock (0.6 mA). A total of 5 tone-shock
631 pairings were delivered with a random inter-tone interval (ITI) of 60-120 seconds. For
632 optogenetic studies, light stimulation occurred only during the 30-second tones of this session.
633 Following delivery of the last foot shock, mice remained in the conditioning chamber for a two
634 minute consolidation period. 24 hours later, mice were placed into a separate conditioning box
635 (Med Associates) that contained a white Plexiglas floor, a striped pattern on the walls, and was
636 cleaned and scented with a 70% EtOH solution. After a 3 minute baseline period, mice were
637 presented with 10 tones (30 seconds, 3 KHz, 80 dB) with a 5 second ITI. Mice remained in the
638 chamber after the last tone for a two-minute consolidation period. 24 hours later (48 hours after
639 training), mice were returned to the original training chamber for 5 minutes. For each session,
640 freezing behavior was hand-scored every 5 seconds by a trained observer blinded to
641 experimental treatment as described previously[24]. Freezing was defined as a lack of movement
642 except as required for respiration.

643 **Immunohistochemistry and histology:** All mice used for behavioral and anatomical tracing
644 experiments were anesthetized with Avertin and transcardially perfused with 30 ml of ice-cold
645 0.01M PBS followed by 30 ml of ice-cold 4% paraformaldehyde (PFA) in PBS. Brains were
646 extracted and stored in 4% PFA for 24 hours at 4°C before being rinsed twice with PBS and

647 stored in 30% sucrose/PBS until the brains sank. 45 μm slices were obtained on a Leica VT100S
648 and stored in 50/50 PBS/Glycerol at -20°C. DREADD or ChR2-containing sections were
649 mounted on slides, allowed to dry, coverslipped with VectaShield (Vector Labs, Burlingame,
650 CA), and stored in the dark at 4°C.

651 *Tryptophan hydroxylase/Fluorogold/cfos triple labeling* We stained free-floating dorsal raphe
652 sections using indirect immunofluorescence sequentially for first tryptophan hydroxylase (TPH)
653 and Fluoro-Gold(FG) and then c-*fos*. For TPH/FG, we washed sections 3X for 5 min with 0.01
654 M PBS, permeabilized them for 30 min in 0.5% Triton/0.01 M PBS, and washed the sections
655 again 2X with 0.01 M PBS. We blocked the sections for 1 hour in 0.1% Triton/0.01 M PBS
656 containing 10%(v/v) Normal Donkey Serum and 1%(w/v) Bovine Serum Albumin (BSA). We
657 then added primary antibodies (1:500 Mouse anti-TPH [Sigma Aldrich T0678] and 1:3000
658 Guinea Pig anti-Fluoro Gold [Protos Biotech NM101]) to blocking buffer and incubated the
659 sections overnight at 4 degrees C. The next day, we washed the sections 3X for 5 min with 0.01
660 M PBS, then incubated them with 1:500 with Alexa Fluor 647-conjugated Donkey anti-mouse
661 and Alexa Fluor 488-conjugated Donkey anti-guinea pig secondary antibodies for 2 hr at RT,
662 and washed the sections 4X for 5 min with 0.01 M PBS. We then proceeded directly to the c-*fos*
663 tyramide signal amplification based immunofluorescent staining. We permeabilized the sections
664 in 50% methanol for 30 min, then quenched endogenous peroxidase activity in 3% hydrogen
665 peroxide for 5 min. Followed by two 10 min washes in 0.01 M PBS, we blocked the sections in
666 PBS containing 0.3% Triton X-100 and 1.0 % BSA for 1 hour. *c-fos* primary antibody (Santa
667 Cruz Biotechnology - sc-52) was added to sections at 1:3000 and sections were incubated for 48
668 hours at 4 degrees. On day 3, we washed the sections in TNT buffer (0.1 M Tris-HCl pH 7.5,
669 0.15 M NaCl, 0.05% Tween-20) for 10 min, blocked in TNB buffer (0.1 M Tris-HCl pH 7.5,

670 0.15 M NaCl, 0.5% Blocking reagent – PerkinElmer FP1020) buffer for 30 min. We then
671 incubated the sections in secondary antibody (Goat anti-rabbit HRP-conjugated- PerkinElmer)
672 1:200 in TNB buffer for 30 min., washed the sections in TNT buffer 4X for 5 min, and then
673 incubated the sections in Cy3 dye diluted in TSA amplification diluents for 10 min. We washed
674 the sections 2X in TNT buffer, mounted them on microscope slides. We coverslipped the slides
675 using Vectashield mounting medium. We acquired 4-5 2x4 tiled z-stack(5 optical slices
676 comprising 7 µm total) images of the dorsal raphe from each naïve and shock mouse on a Zeiss
677 800 Upright confocal microscope. Scanning parameters and laser power were matched between
678 groups. Images were preprocessed using stitching and maximum intensity projection and then
679 analyzed using an advanced processing module in Zeiss Zen Blue that allows nested analysis of
680 multiple segmented fluorescent channels within parent classes. Double and triple-labeled cells
681 were validated in a semi-automated fashion. At least 4 sections per mouse were counted in this
682 way. One mouse was identified as a significant outlier in the Shock group and was excluded
683 from further analysis.

684 *Sert*^{Cre}::ChR2*, and Crf*$^{Intrsect\text{-}ChR2}$ validation: To verify expression of ChR2-expressing fibers in
685 the BNST originating from DR serotonergic neurons, 300 µm slices used for *ex vivo*
686 electrophysiological recordings containing the DR and BNST were stored in 4%
687 paraformaldehyde at 4°C for 24 hours before being rinsed with PBS, mounted, and coverslipped
688 with Vectashield mounting medium. Images showing eYFP fluorescence from the DR and
689 BNST were obtained on a Zeiss 800 upright confocal microscope using a 10x objective and tiled
690 z stacks. To validate the INTRSECT construct, mice received injections of HSV-hEF1α-
691 mCherry or HSV-ef1α-LSL1-mCherry-IRES-flpo to both the LH and VTA bilaterally (N=4 and
692 5, respectively). Both groups received AAVDJ-hSyn-Cre-on/Flp-off-hChR2(H134R)-EYFP to

693 the BNST bilaterally. Six weeks following injection, mice were perfused and tissue was
694 collected as described above. To visualize YFP expression in the BNST of *Crf*^{Cre}::Intrsect^{BNST}
695 mice, free floating slices containing the BNST were rinsed three times with PBS for 5 minutes
696 each. Slices were then incubated in 50% methanol for 30 minutes then incubated in 3% hydrogen
697 peroxide for 5 minutes. Following three 10-minute washes in PBS, slices were incubated in 0.5%
698 Triton X-100 for 30 minutes followed by a 10 minute PBS wash. Slices were blocked in 10%
699 normal donkey serum/0.1% Triton X-100 for 1 hour, and then they were incubated overnight at
700 4°C with a primary chicken anti-GFP antibody (GFP-1020, Aves) at 1:500 in blocking solution.
701 Following primary incubation, slices were rinsed three times with 0.01M PBS for 10 minutes
702 each and incubated with a fluorescent secondary antibody (AlexaFluor 488 Donkey anti-chicken)
703 at 1:200 in PBS for 2 hours at room temperature. Slices were then rinsed with four 10-minute
704 PBS washes before being mounted onto glass slides and coverslipped with Vectashield with
705 DAPI. A 3x4 tiled z stack (7 optical sections comprising 35 μm total) image from both the left
706 and right hemispheres of the BNST was obtained at 20x magnification using a Zeiss 800 upright
707 confocal microscope. Scanning parameters and laser power were matched between groups.
708 Images were preprocessed using stitching and maximum intensity projection. The number of
709 fluorescent cells in the dorsal and ventral aspects of the BNST were counted by a blinded scorer
710 using the cell counter plug-in in FIJI (ImageJ). Each hemisphere was considered independently
711 per mouse. One mouse in the flp-expressing group was a significant outlier for number of cells
712 expressed in a ventral BNST hemisphere (ROUT, Q=0.1%) and all data from that mouse were
713 excluded.

714 *Choleratoxin retrograde tracer studies in CRF reporter mice:* 3 male CRF-L10a reporter mice
715 were injected with 200 nl of CTB 555 and CTB 647 bilaterally to the LH and VTA, respectively,

716 as described above. 5 days following injection, mice were perfused as described above, the
717 brains were extracted, and were stored in 4% paraformaldehyde for 24 hours at 4°C before being
718 rinsed with PBS and transferred to 30% sucrose until the brains sank. 45 μm sections containing
719 the BNST were collected as described above. Sections containing the BNST were mounted on
720 glass slides and coverslipped using Vectashield. An image from the left and right hemispheres of
721 a medial section of the BNST was obtained on a Zeiss 800 upright microscope using a 20x
722 objective and 3x5 tiled z stacks (5 optical slices comprising 7 μm total). Images were
723 preprocessed using stitching and maximum intensity projection, and were then analyzed using
724 the cell counter function in FIJI (ImageJ). Only cells positive for GFP (putative CRF neurons)
725 were considered. Cells were scored exclusively as either 555+ only (LH-projecting), 647+ only
726 (VTA-projecting), 555+ and 647+ (projecting to both LH and VTA), or 555- and 647-
727 (unlabeled; neither LH- nor VTA- projecting). The total number of CRF neurons scored was
728 calculated as the sum of all four groups, and percentages of each type were calculated from this
729 value. Each hemisphere was scored and plotted independently (N=6 images from 3 mice), and
730 the dorsal and ventral BNST were considered separately. The average values were plotted as pie
731 charts (ED 9).

732 **Double Fluorescence *in situ* hybridization (FISH):** For validation of 2C-cre line and
733 comparison of CRF/2C mRNA cellular colocalization, mice were anesthetized using isoflurane,
734 rapidly decapitated, and brains rapidly extracted. Immediately after removal, the brains were
735 placed on a square of aluminum foil on dry ice to freeze. Brains were then placed in a -80°C
736 freezer for no more than 1 week before slicing. 12 μm slices were made of the BNST on a Leica
737 CM3050S cryostat (Germany) and placed directly on coverslips. FISH was performed using the
738 Affymetrix ViewRNA 2-Plex Tissue Assay Kit with custom probes for CRF, 5-HT2C, and Cre

739 designed by Affymetrix (Santa Clara, CA). Slides were coverslipped with SouthernBiotech
740 DAPI Fluoromount-G. (Birmingham, AL). 3x5 tiled z stack (15 optical sections comprising 14
741 µm total) images of the entire 12 µm slice were obtained on a Zeiss 780 confocal microscope for
742 assessment of CRF/2C colocalization. A single-plane 40x tiled image of a CRF/2C slice was
743 obtained on a Zeiss 800 upright confocal microscope for the magnified image shown in Extended
744 Data 6b, right. 3x5 tiled z stack (7 optical sections comprising 18 µm) images of 2C/Cre slices
745 were obtained on a Zeiss 800 upright confocal microscope for the 2C/Cre validation. All images
746 were preprocessed with stitching and maximum intensity projection. An image of the BNST
747 from 3 mice in each condition was hand counted for each study using the cell counter plugin in
748 FIJI (ImageJ). Cells were classified into three groups: probe 1+, probe 2+, or probe 1 and 2 +.
749 Only cells positive for a probe were considered. Results are plotted as average classified
750 percentages across the three images.

751 **Group assignment:** No specific method of randomization was used to assign groups. Animals
752 were assigned to experimental groups so as to minimize the influence of other variables such as
753 age or sex on the outcome.

754 **Inclusion/exclusion criteria:** Pre-established criteria for excluding mice from behavioral
755 analysis included 1) missed injections, 2) anomalies during behavioral testing, such as mice
756 falling off the elevated plus maze, 3) damage to or loss of optical fibers, 4) statistical outliers, as
757 determined by the Grubb's test.

758 **Sample size:** A power analysis was used to determine the ideal sample size for behavior
759 experiments**.** Assuming a normal distribution, a 20% change in mean and 15% variation, we
760 determined that we would need 8 mice per group. In some cases, mice were excluded due to

761 missed injections or lost optical fibers resulting in fewer than 8 mice per group. For
762 electrophysiology experiments, we aimed for 5-7 cells from 3-4 mice.

763 **Statistics:** Data are presented as means ± SEM. For comparisons with only two groups, *p* values
764 were calculated using paired or unpaired t-tests as described in the figure legends. Comparisons
765 across more than two groups were made using a one-way ANOVA, and a two-way ANOVA was
766 used when there was more than one independent variable. A Bonferonni posttest was used
767 following significance with an ANOVA. In cases in which ANOVA was used, the data met the
768 assumptions of equality of variance and independence of cases. If the condition of equal
769 variances was not met, Welch's correction was used. Some of the sample groups were too small
770 to detect normality (<8 samples) but parametric tests were used because nonparametric tests lack
771 sufficient power to detect differences in small samples (Graphpad Statistics Guide –
772 www.graphpad.com). The standard error of the mean is indicated by error bars for each group of
773 data. Differences were considered significant at *p* values below 0.05. All data were analyzed
774 with GraphPad Prism software.

775 21. Krashes, M. J. *et al*. An excitatory paraventricular nucleus to AgRP neuron circuit that
776 drives hunger. *Nature* **507,** 238–42 (2014).
777 22. Madisen, L. *et al*. A robust and high-throughput Cre reporting and characterization
778 system for the whole mouse brain. *Nat*. *Neurosci*. **13,** 133–140 (2010).
779 23. Bath, B. D. *et al*. Subsecond adsorption and desorption of dopamine at carbon-fiber
780 microelectrodes. *Anal*. *Chem*. **72,** 5994–6002 (2000).
781 24. Hefner, K. *et al*. Impaired fear extinction learning and cortico-amygdala circuit
782 abnormalities in a common genetic mouse strain. *J*. *Neurosci*. **28,** 8074–8085 (2008).
783

EXTENDED DATA FIGURE LEGENDS

Extended Data Figure 1: *In vivo* recordings in BNST neurons during fear conditioning reveal opposite patterns of activation during acquisition and recall. (a) Representative neuron firing rate and (b) population Z score of the firing rate for BNST neurons (n=45 cells from 7 mice) 30 s before conditioned stimulus (tone), during the conditioned stimulus, and 30 seconds after the unconditioned stimulus. (c) Percentage time spent freezing during fear acquisition, cued fear recall and contextual fear recall. (d) Electrode placements for BNST recordings. (e) Raw firing rates during freezing (blue) versus movement (red) epochs were averaged across all putative principal neurons (firing rate <10Hz). Acquisition: Cells in BNST exhibited greater average firing rates during freezing epochs compared to movement epochs during CS3 ($t_{44}=2.88$, $p<0.01$, Student's unpaired two-tailed t-test), 4 ($t_{44}=3.14$, $p<0.01$, Student's unpaired two-tailed t-test), and 5 ($t_{44}=4.4$, $p<0.001$, Student's unpaired two-tailed t-test) (n=45 cells from 7 mice). CS Recall: Average firing rates during freezing epochs decreased over CS presentations such that firing during block 5 was significantly less than block 1 ($t_{41}=3.44$, $p=0.001$, Student's unpaired two-tailed t-test). Freezing firing rates during block 5 were also significantly less than movement epochs during block 5 ($t_{41}=4.03$, $p<0.001$, Student's unpaired two-tailed t-test) (n=42 cells from 7 mice). CX test: Average firing rate was significantly greater during movement versus freezing epochs during minutes 1 ($t_{44}=4.83$, $p<0.001$, Student's unpaired two-tailed t-test), 2 ($t_{44}=3.17$, $p<0.01$, Student's unpaired two-tailed t-test), and 5 ($t_{44}=4.36$, $p<0.001$, Student's unpaired two-tailed t-test) (n=45 cells from 7 mice). (f) Freezing-related changes in firing rates during the CS were determined by measuring the ratio of average firing rates during freezing versus movement epochs for each session. Acquisition: Activity during freezing epochs increased significantly relative to movement epochs during CS4

807 (t_{45}=3.26, p<0.01, Student's unpaired two-tailed t-test) and CS5 (t_{45}=2.17, p<0.05, Student's
808 unpaired two-tailed t-test) (n=46 cells from 7 mice). CS Recall: Freezing significantly
809 suppressed activity relative to movement epochs during the last two CS presentations (t_{47}=5.29,
810 p=<0.001, Student's unpaired two-tailed t-test) (n=48 cells from 7 mice) CX test: Freezing
811 significantly suppressed activity during minutes 1 (t_{44}=6.06, p<0.001, Student's unpaired two-
812 tailed t-test), 2 (t_{44}=2.92, p<0.01, Student's unpaired two-tailed t-test), and 5 (t_{44}=3.55, p=.001,
813 Student's unpaired two-tailed t-test) (n=45 cells from 7 mice). (g) Plots showing correlation
814 between freezing behavior and firing rate of BNST neurons across sessions and for all sessions.
815 Data are mean ± s.e.m. *P<0.05 **P<0.01; ***P<0.001. Scale bar = 100 µm.

816

817 **Extended Data Figure 2: Effects of optogenetic stimulation of 5HT inputs to the BNST on**
818 **feeding, anxiety and locomotion.** (a-c) $Sert^{Cre}$::$ChR2^{DRN\rightarrow BNST}$ mice exhibited reduced
819 probability (t_{15}=2.67, p<0.05, Student's unpaired two-tailed t-test, n=8 control, n=9 ChR2) and
820 latency (t_{15}=1.003, p>0.05, Student's unpaired two-tailed t-test, n=8 control, n=9 ChR2) to enter
821 the open arms of the EPM without exhibiting locomotor deficits. (d) Photostimulation of 5-
822 $HT^{DRN\rightarrow BNST}$ terminals had no effect on locomotor activity in the open field (n=9 control, n=11
823 ChR2) or (e) home cage feeding (n=4 control, n=6 ChR2). Data are mean ± s.e.m. *P<0.05.

824

825 **Extended Data Figure 3: Chemogenetic activation of 5-HT$_{2C}$R expressing neurons in the**
826 **BNST increases anxiety-like behavior.** (a) Confocal images of coronal BNST slices obtained
827 from *htr2c*^{Cre} mice following double fluorescence in situ hybridization for 5-HT$_{2C}$R and cre.
828 Yellow arrows indicate cells in which there is colocalization, red arrows indicate cells in which
829 only Cre is expressed and green arrows indicate cells in which only 5-HT$_{2C}$R is expressed. (b)

830 Pie chart representing the distribution of genetic markers in BNST neurons. (c) Experimental
831 configuration in *Htr2c*^{cre}::hM3Dq^{BNST} mice. (d) Coronal images showing cfos induction in 5-
832 HT_{2C}R expressing neurons in the BNST of *Htr2c*^{Cre}::hM3Dq^{BNST} or *Htr2c*^{Cre}::mCherry^{BNST} mice
833 following CNO injection. (e) Bath application of CNO depolarized 5HT_{2C}R-expressing neurons
834 expressing hM3Dq in slice (n=3 cells from 3 mice). (f) Chemogenetic stimulation of 5-HT_{2C}R
835 expressing neurons in BNST increased latency to feed in the NSF ($t_{11}=2.591$, $p<0.05$, Student's
836 unpaired two-tailed t-test, n=6; mCherry, n=7 hM3Dq). (g) Chemogenetic activation of 5-
837 HT_{2C}R-expressing BNST neurons had no effect on home cage feeding (n=5 mCherry, n=6
838 hM3Dq). (h) Confocal images from *Htr2c*^{Cre}::mCherry^{BNST} mice showing mCherry expression in
839 5-HT_{2C}R-expressing soma in the BNST and fibers in the LH and VTA. Data are mean ± s.e.m.
840 *P<0.05. Scale bar = 100 μm.
841
842 **Extended Data Figure 4: Electrophysiological characterization of 5-HT responses and 5-**
843 **HT receptor expression in CRF^{BNST} neurons** (a) A pie chart showing the distribution of
844 CRF^{BNST} neurons that were depolarized, hyperpolarized, or had no response to 5-HT (n=8 cells
845 from 4 mice). (b) Coronal images of the BNST showing colocalization of 5-HT_{2C}Rs with CRF
846 mRNA using double fluorescence *in situ* hybridization and (c-d) histograms showing the % of 5-
847 HT_{2C} neurons that express CRF and the % of CRF neurons that express 5-HT_{2C}Rs in the BNST
848 (n=3 slices from 3 mice). (e) Recording configuration in CRF^{BNST} neurons. (f) Slice
849 electrophysiology in BNST of *Crf* reporter mice showing depolarization of all (VTA-projecting
850 and non-projecting) CRF neurons following bath application of the 5-HT_2 receptor agonist
851 mCPP (n=12 cells from 6 mice) and blockade of this response by the 5-HT_{2C} receptor antagonist
852 RS 102221 (n=5 cells from 3 mice). (g) Change in membrane potential induced by mCPP

853 (t_{12}=2.18, p<0.05, One-sample t-test, n=12 cells from 6 mice) is blocked by a 5-HT$_{2C}$R
854 antagonist (n=5 cells from 3 mice). (h) mCPP selectively depolarizes non-VTA projecting
855 CRF^{BNST} neurons (n=3 cells from 2 mice non VTA-projecting CRF, n=5 cells from 4 mice VTA-
856 projecting CRF). Data are mean ± s.e.m. *P<0.05.
857
858 **Extended Data Figure 5: 5-HT activates inhibitory microcircuits in the BNST that**
859 **modulate outputs to the LH.** (a) Recording configuration in CRF reporter mice infused with
860 retrograde tracer beads in the LH. (b) Average traces of 5-HT induced depolarization in LH
861 projecting vs non-projecting neurons (c) Histograms showing 5-HT induced depolarization in
862 non-LH projecting BNST neurons (t_4=4.425, p<0.05, One-sample t-test, n=5 cells from 3 mice)
863 and hyperpolarization in LH-projecting neurons (t_5=2.789, p<0.05, One-sample t-test, n=6 cells
864 from 3 mice). (d) Confocal image of retrogradely CTB-labeled VTA (red) and LH (green)
865 outputs in a *CRF-L10a* reporter (blue). (e-f) Pie charts depicting the percentage of LH-projecting
866 only, VTA-projecting only, collateralizing, and CTB-negative (unlabeled) CRF in neurons in the
867 dorsal and ventral aspects of the BNST (n=6 hemispheres from 3 mice). (g) Experimental
868 schematic depicting viral infusions into the BNST and retrograde tracer bead infusions into the
869 LH of *Crf*^{Cre}::ChR2^{BNST} mice. (h) Recording configuration in *Crf*^{Cre}::ChR2^{BNST} mice with LH
870 tracer beads (i) Representative trace of light evoked IPSCs in LH projecting neurons (n=7 cells
871 from 4 mice) and blockade of this light evoked response by GABAzine (n=2 cells from 2 mice).
872 (j) Recording configuration in VTA projecting neurons in the BNST of C57BL/6 mice. (k-l) 5-
873 HT has no effect on miniature IPSC frequency or amplitude in BNST→VTA projecting neurons
874 (n=7 from 4 mice). (m-n) 5-HT has no effect on sIPSC frequency or amplitude in the presence of
875 the 5-HT$_{2C}$R antagonist RS102221 (n=5 cells from 4 mice). (o) Recording configuration in LH

876 projecting neurons in the BNST of C57BL/6 mice (p) Representative traces showing an increase
877 in sIPSC frequency in the presence of 5-HT for 6 cells from 3 mice (q-r) 5-HT increases sIPSC
878 frequency but not amplitude in BNST→LH projecting neurons ($F_{11,55}$=11.65, p<0.01, Repeated
879 measures one-way ANOVA, n=6 cells from 3 mice). (s-t) 5-HT has no effect on miniature IPSC
880 frequency or amplitude (n=5 cells from 3 mice). (u-v) 5-HT has no effect on sIPSC frequency or
881 amplitude in the presence of RS102221 (n=6 cells from 4 mice). Data are mean ± s.e.m.
882 *P<0.05.

883

884 **Extended Data Figure 6: 5-HT does not alter GABAergic transmission in CRF neurons nor**
885 **does it directly excite non-CRF VTA projecting neurons in the BNST.** (a) Recording
886 configuration in CRF^{BNST} neurons in a CRF reporter. (b-c) 5-HT has no effect on sIPSC
887 frequency or amplitude in the total population of CRF neurons (n=5 cells from 3 mice). (d)
888 Recording configuration in non-CRF, VTA projecting neurons in the BNST and average trace of
889 5-HT effect on membrane potential in non-CRF, VTA projecting neurons in the presence of
890 TTX. (e) Histogram summarizing 5-HT effects on membrane potential in local and VTA
891 projecting CRF neurons and local CRF neurons in the presence of the 5-HT_{2C} receptor antagonist
892 RS102221 (same data shown in Figure 2b) juxtaposed with the lack of effect of 5-HT on
893 membrane potential in non-CRF, VTA projecting neurons (t_4=0.9381, ns, One-sample t-test, n=5
894 cells from 3 mice). Data are mean ± s.e.m. **P<0.01; ***P<0.001.

895

896 **Extended Data Figure 7: The 5-HT_2 agonist mCPP increases GABAergic but not**
897 **glutamatergic transmission in the BNST.** (a-b) mCPP increases sIPSC frequency
898 ($F_{15,30}$=1.863, p<0.001, Repeated measures one-way ANOVA, n=3 cells from 3 mice) but not

899 amplitude in the BNST of C57BL/6 mice. (c-d) mCPP has no effect on sEPSC frequency or
900 amplitude in the BNST of C57BL/6 mice (n=5 cells from 3 mice). Data are mean ± s.e.m.
901 *P<0.05.

902

903 **Extended Data Figure 8: Optogenetic and Intrsectional characterization of 5-HT-CRF**
904 **circuits in the BNST and outputs to the midbrain** (a) Experimental design and recording
905 configuration from *Sert*^{Cre}::ChR2$^{DRN\rightarrow BNST}$ mouse with retrograde tracer beads in the VTA. (b)
906 Representative traces for 5 cells from 3 mice depicting the increase in sIPSCs in VTA projecting
907 neurons in the BNST following light-evoked 5-HT release (c) Histogram summarizing the effect
908 of light evoked 5-HT release on sIPSC frequency in VTA projecting neurons (t_4=4.890, p<0.01,
909 One-sample t-test, n=5 cells from 3 mice). (d) Experimental configuration in *Crf*^{Cre}::Intrsect-
910 ChR2^{BNST} mice. (e) Representative images from 4 *Crf*^{Cre}::HSV-LSL1-mCherry-flpo$^{VTA/LH}$ mice
911 and 4 *Crf*^{Cre}::HSV-LSL1-mCherry$^{VTA/LH}$ mice injected with Intrsect-ChR2-eYFP in the BNST.
912 (f) Cell counts of eYFP+ neurons from HSV-LSL1-flpo and HSV-LSL1-mCherry injected
913 *Crf*^{Cre}::Intrsect-ChR2^{BNST} mice indicating the number of non-projecting CRF neurons compared
914 to the total CRF population in the dorsal (top panel; t_{14}=1.959, ns, Student's unpaired two-tailed
915 t-test, n=4 mice, 8 hemispheres per group) and ventral aspects of the BNST (bottom panel;
916 t_7=2.431, p<0.05, Student's unpaired Welch's corrected two-tailed t-test, n=4 mice, 8
917 hemispheres per group) (g) Recording configuration and light evoked IPSC showing local
918 GABA release from non-projecting CRF neurons in the BNST. (h) Sterotaxic injection of ChR2
919 in *Crf*^{cre} mouse (i-j) Light evoked IPSCs in the VTA and LH indicating that CRF projections to
920 these regions are GABAergic. Data are mean ± s.e.m. *P<0.05; **P<0.01.

921

922 **Extended Data Figure 9: Pharmacological blockade of CRF_1 receptors reduces fluoxetine**
923 **induced aversive behavior and 5-HT enhancement of GABAergic transmission in the**
924 **BNST.** (a) Experimental schedule of injections and behavior. (b) CRF_1R antagonist does not
925 modify fear acquisition but reduces fluoxetine enhancement of cued fear recall ($F_{1,20}=13.70$,
926 $p<0.01$, Two-way ANOVA, n=6 per group). (c) Recording configuration in BNST neurons that
927 project to the LH in C57BL/6 mice. (d) Bath application of a CRF_1R antagonist blocks the 5-HT
928 induced increase in sIPSC frequency in LH projecting neurons in the BNST ($F_{10,30}=0.2213$, ns,
929 Repeated measures one-way ANOVA, n=4 cells from 2 mice). (e) There was a reduction in
930 sIPSC amplitude during 5-HT bath application and CRF_1R blockade ($F_{10,30}=2.941$, $p<0.05$,
931 Repeated measures one-way ANOVA, n=4 cells from 2 mice). Data are mean ± s.e.m. **P<0.01.

932

933 **Extended Data Figure 10: Model of a serotonin-sensitive inhibitory microcircuit in the**
934 **BNST that modulates anxiety and aversive learning.** Serotonin inputs to the BNST activate 5-
935 $HT_{2C}Rs$ expressed in non-projecting "local" CRF neurons. These "local" CRF neurons promote
936 anxiety and fear by inhibiting anxiolytic outputs to the VTA and LH that are putatively
937 GABAergic. Another discrete subset of CRF neurons, which are inhibited by 5-HT, send direct,
938 inhibitory projections to the VTA and LH. These CRF^{BNST} output neurons are GABAergic and
939 putatively anxiolytic and stress buffering. Blue dashed lines indicate hypothesized additional
940 synapses between CRF^{BNST} neurons. Dashed red line indicates a putatively GABAergic synapse.

941

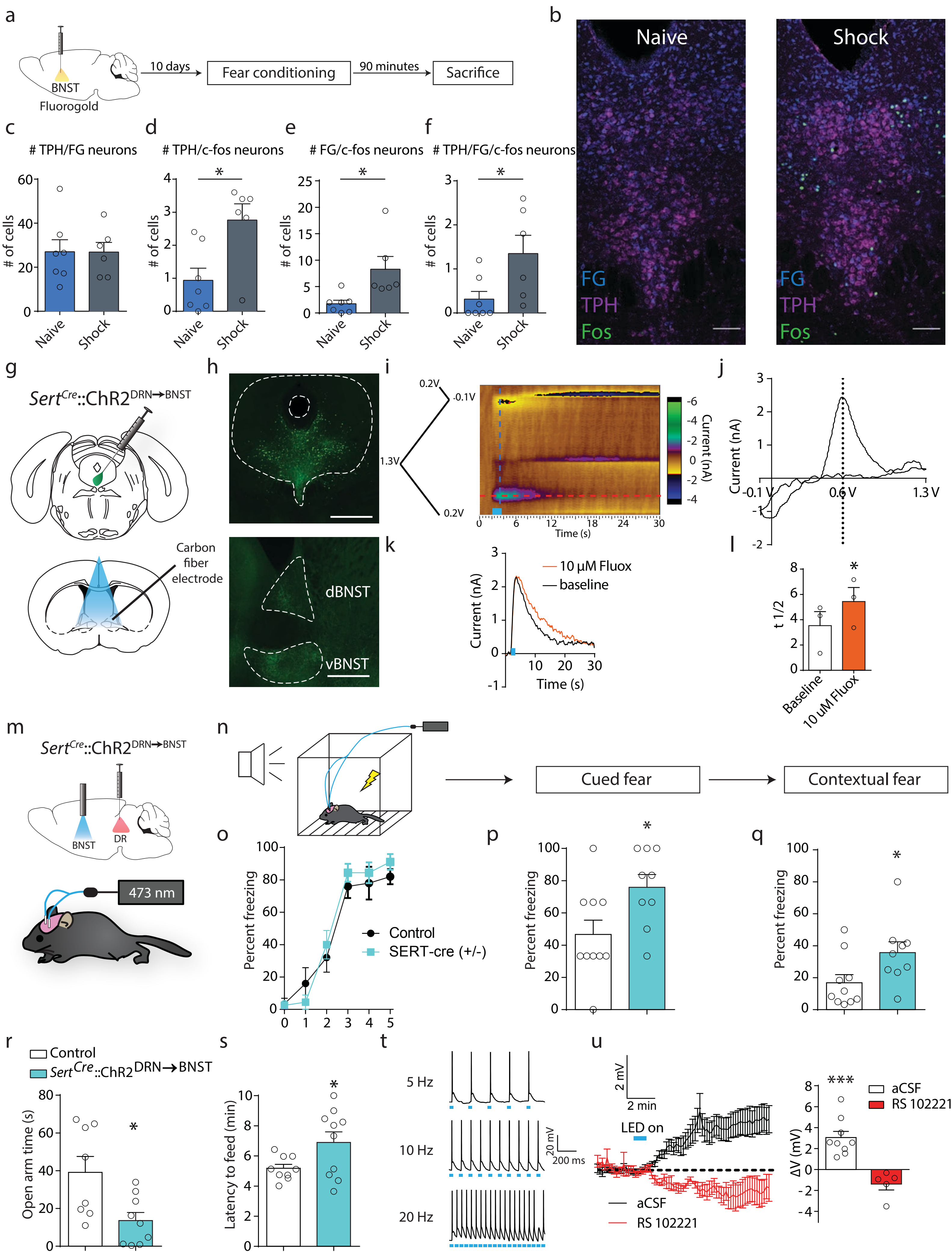

a
BNST
Fluorogold
10 days
Fear conditioning
90 minutes
Sacrifice
b
Naive
Shock
FG
TPH
Fos
c
TPH/FG neurons
d
TPH/c-fos neurons
e
FG/c-fos neurons
f
TPH/FG/c-fos neurons
of cells
Naive
Shock
*
g
SertCre::ChR2DRN→BNST
Carbon fiber electrode
h
dBNST
vBNST
i
0.2V
-0.1V
1.3V
0.2V
Current (nA)
Time (s)
j
Current (nA)
-0.1 V
0.6 V
1.3 V
k
10 µM Fluox
baseline
Current (nA)
Time (s)
l
t 1/2
Baseline
10 uM Fluox
m
SertCre::ChR2DRN→BNST
BNST
DR
473 nm
n
Cued fear
Contextual fear
o
Percent freezing
Control
SERT-cre (+/-)
p
Percent freezing
q
Percent freezing
r
Control
SertCre::ChR2DRN→BNST
Open arm time (s)
s
Latency to feed (min)
t
5 Hz
10 Hz
20 Hz
20 mV
200 ms
u
2 mV
2 min
LED on
aCSF
RS 102221
ΔV (mV)
***

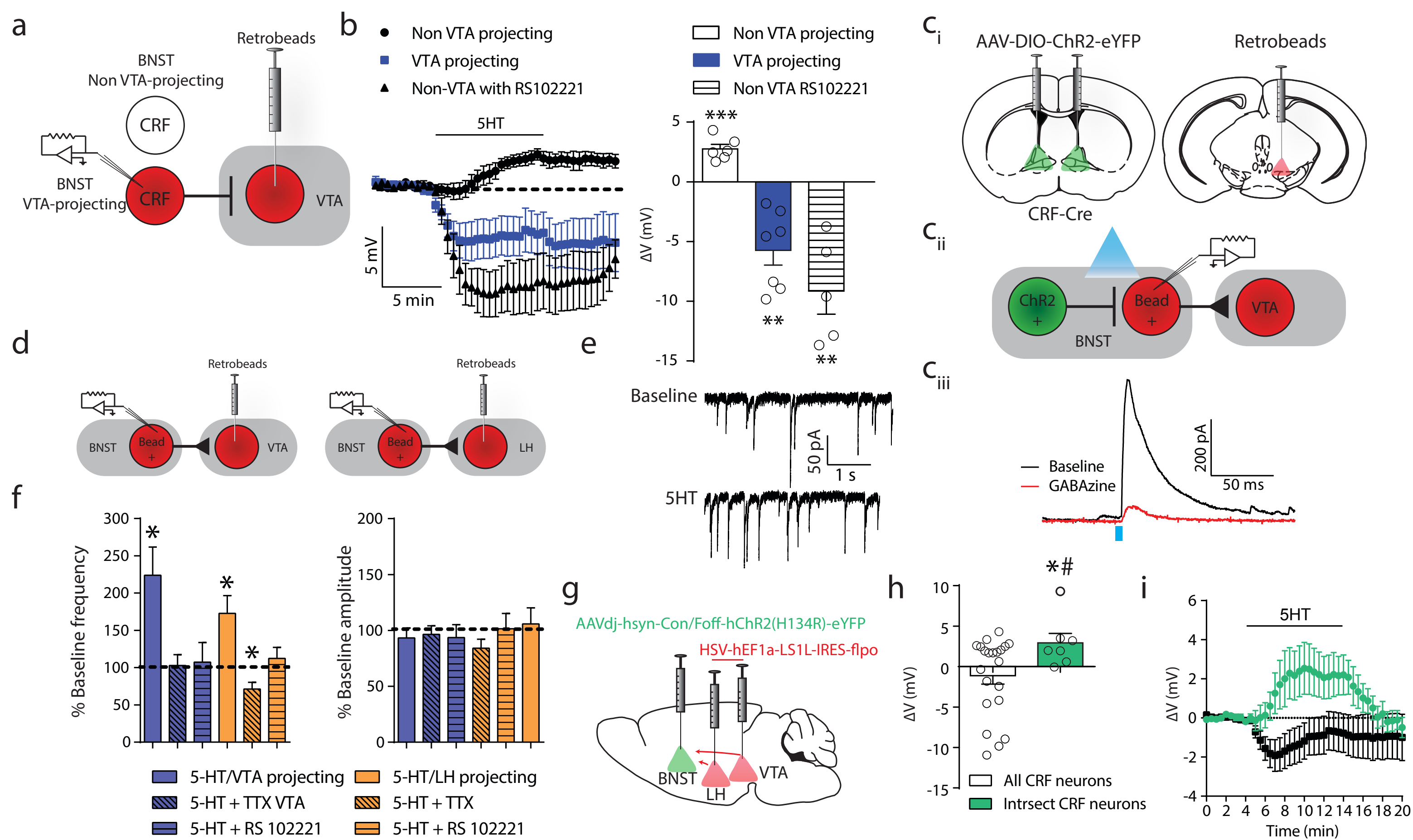
a
Retrobeads
BNST
Non VTA-projecting
CRF
BNST
VTA-projecting
CRF
VTA
b
Non VTA projecting
VTA projecting
Non-VTA with RS102221
5HT
5 mV
5 min
Non VTA projecting
VTA projecting
Non VTA RS102221
ΔV (mV)
AAV-DIO-ChR2-eYFP
Retrobeads
CRF-Cre
ChR2
Bead
BNST
VTA
Baseline
GABAzine
200 pA
50 ms
d
Retrobeads
BNST
Bead
VTA
LH
e
Baseline
5HT
50 pA
1 s
f
% Baseline frequency
% Baseline amplitude
5-HT/VTA projecting
5-HT + TTX VTA
5-HT + RS 102221
5-HT/LH projecting
5-HT + TTX
5-HT + RS 102221
g
AAVdj-hsyn-Con/Foff-hChR2(H134R)-eYFP
HSV-hEF1a-LS1L-IRES-flpo
BNST
LH
VTA
h
ΔV (mV)
All CRF neurons
Intrsect CRF neurons
i
5HT
ΔV (mV)
Time (min)

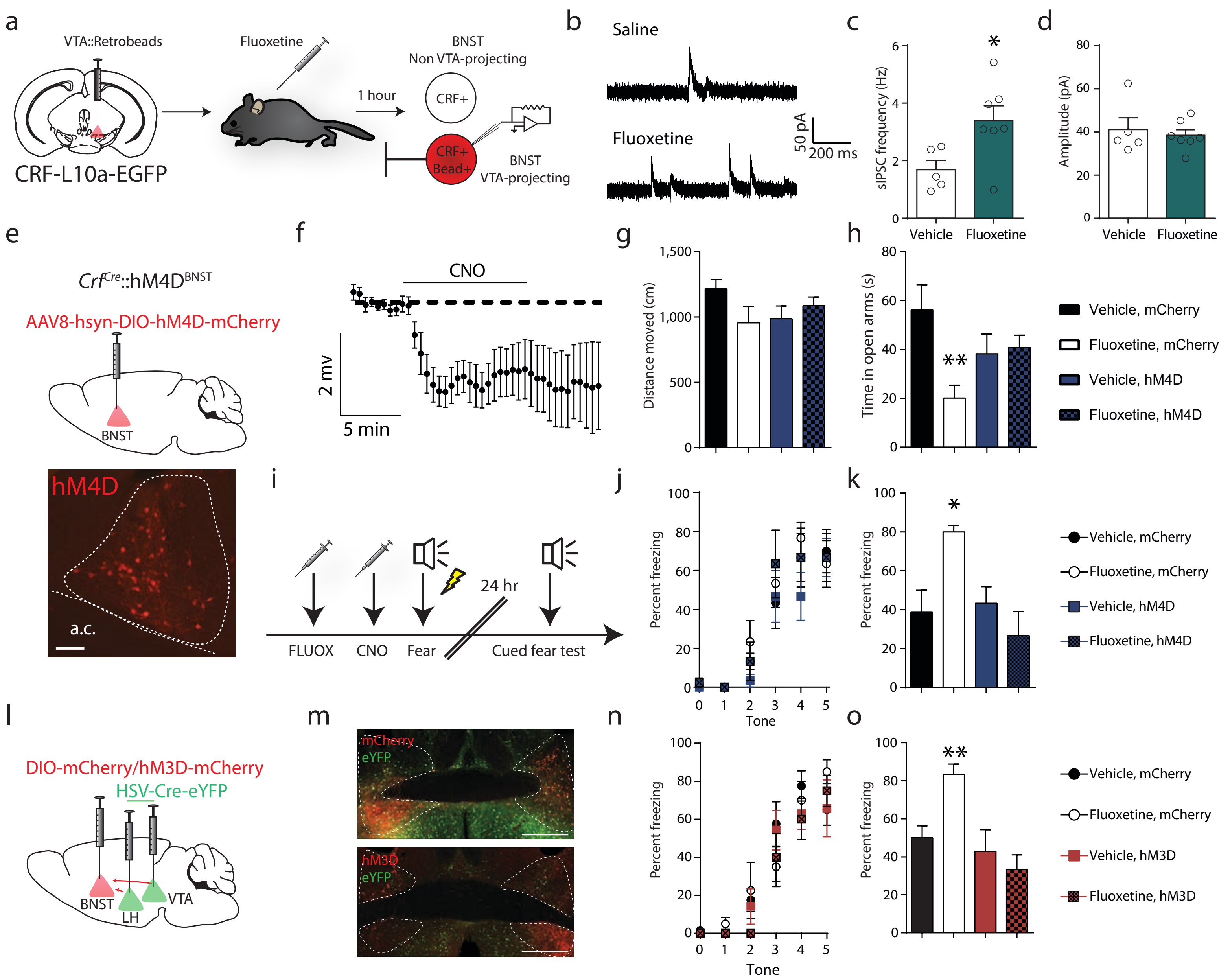
a
VTA::Retrobeads
Fluoxetine
BNST
Non VTA-projecting
1 hour
CRF+
CRF+
Bead+
BNST
VTA-projecting
CRF-L10a-EGFP
b
Saline
Fluoxetine
50 pA
200 ms
c
sIPSC frequency (Hz)
Vehicle
Fluoxetine
*
d
Amplitude (pA)
Vehicle
Fluoxetine
e
Crf^Cre::hM4D^BNST
AAV8-hsyn-DIO-hM4D-mCherry
BNST
hM4D
a.c.
f
CNO
2 mv
5 min
g
Distance moved (cm)
h
Time in open arms (s)
**
Vehicle, mCherry
Fluoxetine, mCherry
Vehicle, hM4D
Fluoxetine, hM4D
i
FLUOX
CNO
Fear
24 hr
Cued fear test
j
Percent freezing
Tone
k
Percent freezing
*
Vehicle, mCherry
Fluoxetine, mCherry
Vehicle, hM4D
Fluoxetine, hM4D
l
DIO-mCherry/hM3D-mCherry
HSV-Cre-eYFP
BNST
LH
VTA
m
mCherry
eYFP
hM3D
eYFP
n
Percent freezing
Tone
o
Percent freezing
**
Vehicle, mCherry
Fluoxetine, mCherry
Vehicle, hM3D
Fluoxetine, hM3D